

MODELING SULFATE-REDUCING PERMEABLE REACTIVE BARRIERS FOR TREATMENT OF ACID MINE DRAINAGE¹

Paulo S. Hemsí², Charles D. Shackelford, and Linda A. Figueroa

Abstract. The performance of sulfate-reducing permeable reactive barriers (PRB) used for the treatment of acid-mine drainage is critically affected by kinetics of cellulose decomposition and substrate production, as well as by kinetics of sulfate reduction and methanogenesis. When biofilm models are considered, the rate of substrate diffusion into the biofilm also affects performance. In this regard, results from an algorithm adapted to simulate the kinetics of the processes occurring in the PRB environment for the purpose of design and evaluation of PRBs are presented. The processes considered include solid organic-matter decomposition, glucose fermentation to acetate (the microbial substrate), sulfate reduction, precipitation of heavy metals as insoluble sulfides, and methanogenesis. Knowledge of the composition of the reactive mixture within the PRB is a prerequisite for modeling cellulose degradation, especially in terms of parameter estimation. Preliminary modeling results for batch (no-flow) conditions reveal issues of practical importance in the design of sulfate-reducing permeable reactive barriers, such as restrictions in PRB performance due to slow kinetics of cellulose decomposition, and due to competition between sulfate reducers and methanogens for acetate.

Key Words: sulfate reduction, ground water, remediation, bioremediation.

¹Paper was presented at the 2003 National Meeting of the American Society of Mining and Reclamation and the 9th Billings Land Reclamation Symposium, Billings MT, June 3-6, 2003. Published by ASMR, 3134 Montavesta Rd., Lexington, KY 40502.

²Paulo S. Hemsí is a Graduate Student, Department of Civil Engineering, Colorado State University, Fort Collins, CO 80523-1372, pshemsi@engr.colostate.edu. Charles D. Shackelford is a Professor, Department of Civil Engineering, Colorado State University. Linda A. Figueroa is an Associate Professor, Department of Environmental Science and Engineering, 1500 Illinois, Coolbaugh Hall, Colorado School of Mines, Golden, CO 80401-1887.

Proceedings American Society of Mining and Reclamation, 2003 pp 367-386

DOI: 10.21000/JASMR03010367

<https://doi.org/10.21000/JASMR03010367>

Introduction

Permeable reactive barriers (PRBs) have the potential to remediate ground water contaminated by acid-mine drainage (AMD), which is characterized by high sulfate and metals concentrations and low pH. Permeable reactive barriers containing either zero-valent iron (e.g., Bain et al., 2002), or solid organic-carbon (e.g., Waybrant et al., 2002) have been considered as suitable for treating AMD. The focus of this paper is on solid organic carbon PRBs that treat AMD through the process of sulfate reduction.

Sulfate-reducing PRBs promote the removal of different inorganic contaminants from contaminated ground water by means of biologically-mediated reactions, resulting in the precipitation of heavy metals as insoluble metal sulfides (biotransformation), as well as the removal of sulfate, and the amelioration of solution pH. In the study of sulfate-reducing PRBs, slow kinetics of cellulose (i.e., solid organic-matter) decomposition, and the competition between sulfate reducers and methanogens, can be restrictive to the treatment efficiency. As a result, predictive numerical models can be used to assess the performance of sulfate-reducing PRBs for a variety of conditions. Thus, the ultimate goal of this research is to develop numerical models for the design and evaluation of sulfate-reducing PRBs for treatment of AMD.

Composition of the Mixture

As shown in Table 1, a variety of reactive-mixture compositions has been reported for batch and column experiments simulating sulfate-reducing PRBs for AMD remediation. All of the compositions shown in Table 1 include three primary components: (i) organic materials, (ii) granular materials, and (iii) limestone.

The organic materials, ranging from leave compost to sewage sludge, act as sources of degradable cellulose and other biopolymers, providing the organic substrate required for the activity of sulfate-reducing bacteria. The granular materials (e.g., pea gravel and sand) are required to maintain a sufficiently high hydraulic conductivity for the PRB. Limestone is used to buffer the initially low pH in the AMD to some higher value within the barrier.

An ideal organic mixture comprises organic materials of different degradability, including materials that degrade more readily to initiate the process, such as alfalfa and leaf compost, and

materials that degrade relatively slowly, such as wood chips and sawdust, to provide for greater persistence or longevity within the barrier. As a result, any mathematical algorithm of cellulose degradation in sulfate-reducing PRBs needs to contain the ability to evaluate a variety of possible degradation rates.

Table 1. Composition of organic reactive mixtures in column tests simulating sulfate-reducing permeable reactive barriers (v = volume, m = mass).

<u>Component</u>	<u>Component Composition (%)</u>				
	(v/v)	(m/m)	(m/m)	(v/v)	(v/v)
Leaf compost or Alfalfa	20	20	23	10	15
Municipal compost or Farm manure	20	-	-	25	-
Sawdust	-	10	22	15	-
Wood chips	9	8	-	-	-
Sewage sludge	-	10	-	-	-
Pea gravel or creek sediment	50	43	44	-	84
Silica sand	-	7	8	-	-
Limestone	1	2	3	50	1
Reference	Benner et al. (1999)	Waybrant et al. (2002)	Waybrant et al. (2002)	Gilbert et al. (1999)	Ludwig et al. (2002)

Kinetic Model of Cellulose Decomposition

Sulfate-reducing bacteria require a dissolved organic substrate as an energy and carbon source for growth (electron donor in sulfate reduction), and the production of this substrate in solution depends on the break down of organic materials in the reactive mixture. The reactive mixture contains solid particulate organic matter in which cellulose (large carbohydrate polymer) can be degraded, or hydrolyzed, to smaller molecules, and subsequently glucose. Glucose can be fermented to organic acids, which are the major energy substrates to the sulfate reducers

(Ingvorsen et al., 1984; Schönheit et al., 1982). Acetate was selected as the model organic acid because both sulfate reducers and methanogens can use acetate for growth.

Among several models describing cellulose decomposition (e.g., Humphrey 1979, Janssen 1984, Drury 2000, Westrich and Berner 1984), the model presented in this paper was based on the assumptions made by Humphrey (1979), and also used by Ladisch et al. (1981). In this model, hydrolysis of cellulose to cellobiose is a heterogeneous reaction involving enzyme adsorption onto the surface of cellulose particles, and the subsequent reaction from cellobiose to glucose takes place in the solution phase. The rate of polymer (cellulose, C) hydrolysis to cellobiose (C_b) is proportional to the concentrations of adsorbed enzyme (E_{ads}) and of cellulose, and is considered product inhibited, as follows:

$$\frac{dC}{dt} = -kE_{ads}C \frac{I}{I + C_b} \quad (1)$$

where k is the hydrolysis rate coefficient, and I is the cellobiose inhibition coefficient. The concentration E_{ads} can be related to the enzyme concentration in solution by a Langmuir isotherm as follows:

$$E_{ads} = E_{ads}^M \left(\frac{E}{\alpha + E} \right) \quad (2)$$

where E is the enzyme concentration in solution, α is an isotherm coefficient, and E_{ads}^M is the maximum adsorption capacity.

In the present study, the maximum adsorption capacity was expressed in terms of physico-chemical characteristics of cellulose particles as follows:

$$E_{ads}^M = (4\pi r^2)N \cdot d_s \cdot M_{w,E} \quad (3)$$

where r is the radius of spherical cellulose particles, N the number of cellulose particles per unit mass of cellulose, d_s is the number of moles of adsorption sites per unit surface area of cellulose, and $M_{w,E}$ is the molecular weight of the enzyme.

Humphrey (1979) assumed that cellulose particles behave as “shrinking-spheres”, and that cellulose concentration (mass of cellulose per volume of solution) can be expressed as a function of the radius of the cellulose particles at a given time as follows:

$$C = \left(\frac{4}{3}\right)\pi \cdot r^3 \cdot \rho \cdot n \quad (4)$$

where ρ is the cellulose density, and n the number of cellulose particles per unit volume of solution, which is a constant in Humphrey’s model (i.e., particles shrink, but the number of particles per unit volume of solution does not change).

Combining Eqs. 3 and 4, E_{ads}^M is proportional to $C^{2/3}$, as obtained in Ladisch et al. (1981), and upon further substitution into Eq. 1, and also acknowledging that $N = n/C$, the following kinetic expression for cellulose hydrolysis is obtained:

$$\frac{dC}{dt} = -KC^{2/3} \left(\frac{E}{\alpha + E}\right) \left(\frac{I}{I + C_b}\right) \quad (5)$$

where

$$K = 4.836 \cdot k \cdot \left(\rho^{-2/3} n^{1/3} d_s M_{w,E}\right) \quad (6)$$

Equation 5 differs from the expression presented by Humphrey (1979) in that the rate of cellulose hydrolysis is proportional to $C^{2/3}$, instead of $C^{4/3}$ as shown by Humphrey (1979). In reviewing that work, apparently the exponent does not account for the fact that $N = n/C$, as proposed through Eq. 5 in the present study.

The complete kinetic process extends to the production of acetate in solution from solid organic matter hydrolysis, and is illustrated in Figure 1. The expressions for the kinetic rates of production of all components in Figure 1 are given by Eqs. 7 to 12.

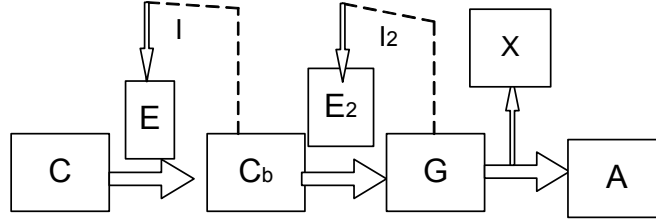


Figure 1. Process from cellulose hydrolysis to acetate production (cellulose (C), cellobiose (C_b), glucose (G), acetate (A), fermenters (X), enzyme 1 (E), and enzyme 2 (E₂), and inhibition factors (I and I₂). Adapted from Humphrey (1979).

The cellulose components are represented as follows:

$$\frac{dC_i}{dt} = -K_i (C)_i^{2/3} \left(\frac{I}{I + C_b} \right) \left(\frac{E}{\alpha + E} \right) \quad (7)$$

where the subscript i accounts for different types of cellulose being degraded. For the intermediate solution products, cellobiose and glucose, the degradation rates are expressed as follows:

$$\frac{dC_b}{dt} = 1.056KC^{2/3} \left(\frac{I}{I + C_b} \right) \left(\frac{E}{\alpha + E} \right) - k_b E_2 \left(\frac{C_b}{K_{C_b} + C_b} \right) \left(\frac{I_2}{I_2 + G} \right) \quad (8)$$

and

$$\frac{dG}{dt} = 1.053k_b E_2 \left(\frac{C_b}{K_{C_b} + C_b} \right) \left(\frac{I_2}{I_2 + G} \right) - 6.078\mu X \left(\frac{G}{K_G + G} \right) \quad (9)$$

where the constants 1.056 and 1.053 are mass yield coefficients from biochemical reactions, μ is the maximum specific growth rate of fermenters, and X is the microbial concentration.

Microbial growth based on glucose is modeled using Michaelis-Menten kinetics (Humphrey 1979) with a decay term of rate d_c , as follows:

$$\frac{dX}{dt} = \mu X \left(\frac{G}{K_G + G} \right) - d_c X \quad (10)$$

The production of enzymes (E and E₂, as shown in Figure 1) is directly linked to microbial kinetics as follows:

$$\frac{dE}{dt} = Y_E \left(\frac{dX}{dt} \right) \quad (11)$$

and

$$\frac{dE_2}{dt} = Y_{E2} \left(\frac{dX}{dt} \right) \quad (12)$$

where Y_E and Y_{E2} are enzyme yield coefficients. Finally, the rate of production of acetate can be quantified from microbial growth:

$$\frac{dA}{dt} = 4.656\mu X \left(\frac{G}{K_G + G} \right) \quad (13)$$

where the constant 4.656 is a mass yield coefficient from the corresponding biochemical reaction. The quantification of acetate production directly from the rate of glucose transformation was also considered in this study (not shown).

Numerical Simulation of Cellulose Decomposition

A Fortran-95 algorithm for the numerical simulation of the system of coupled ordinary differential equations (Eqs. 7 to 13) was developed using the Runge-Kutta-Fehlberg method of numerical integration (Chapra and Canale 2002). Two independent computations of values of the seven variables C, C_b, G, X, E, E₂, and A were obtained at each time level.

Effect of Cellulose Particle Size

The numerical algorithm was employed in example computations to simulate the effect of cellulose particle size during batch experiments (no flow) on the final acetate concentration produced in solution after 720 hours (30 days). Values of initial concentrations (at the beginning of the batch-experiment simulation) were selected, and are shown in Table 2. The initial concentration selected for the microbial population is equivalent to ~10⁵ cells/mL of solution for

cellulolytic bacteria. The initial concentrations of enzymes represent an arbitrarily small, but non-zero value. The hydrolysis products were assumed to be initially not present in solution, and an initial concentration of 3 g/L of cellulose was arbitrarily chosen.

In addition to the yield coefficients included in Eqs. 7 to 13, the values of Y_E and Y_{E2} were adopted as 0.01 and 0.03, respectively (Humphrey 1979). The molecular weight of enzymes was adopted as 400 g/mol, the density of cellulose was adopted as 1000 g/L, and the adsorption-site density on cellulose was considered 10^{-4} moles of adsorption sites per 100 cm² of cellulose. The remaining parameter values adopted in this simulation are shown in Table 3. The selection of values for the rate coefficients k , k_b , and μ took into consideration that the rate coefficient of the heterogeneous reaction involving enzyme adsorption is one order-of-magnitude lower than the rate coefficient of reactions in solution. During the progress of this study, a parametric evaluation based on several different parameter sets was performed, and the results analyzed (not shown).

The effect of cellulose particle size was evaluated by maintaining all other parameters the same, and varying the initial cellulose diameter (Eqs. 4 and 6), in a series of simulations using the Fortran algorithm. For a base simulation with cellulose diameter of 2.0 mm, Figure 2 shows the resulting batch concentrations of the products cellobiose, glucose, and acetate as a function of reaction time.

Table 2. Initial concentrations considered in example simulations.

Component	Initial Concentration (mg/L)
Cellulose	3,000
Cellobiose	zero
Glucose	zero
Fermenters	10
Enzyme 1	0.1
Enzyme 2	0.1
Acetate	zero

Table 3. Adopted parameter values in example simulations.

Relevant Equation	Parameter	Adopted Value
1	k	0.1 hr^{-1}
7	α	2.0 mg/L
7	I	10 mg/L
8	k_b	1.0 hr^{-1}
8	K_{CB}	2.0 mg/L
8	I_2	10 mg/L
9	μ	1.0 hr^{-1}
9	K_G	2.0 mg/L
10	d_c	0.0 hr^{-1}

As shown in Figure 2, the intermediate products (cellobiose and glucose) are progressively fermented to acetate and occur at low concentrations ($< 8 \text{ mg/L}$ for cellobiose, and \sim zero for glucose).

Acetate is accumulated in the batch simulation (to a concentration of $\sim 150 \text{ mg/L}$ at 30 days), simultaneously to the decrease in the concentration of cellulose and to microbial growth (Figure 3).

Following the base simulation, the evaluation of the effect of cellulose particle size was performed considering initial cellulose diameters ranging from 0.5 mm to 30 mm. The resulting acetate 30-day concentrations under batch conditions are shown in Figure 4. Despite variability associated with the choice of the parameter set, simulated values of acetate concentrations reveal a strong dependency on cellulose particle size. The smaller the cellulose particles, the higher the accumulated acetate concentration produced under batch conditions (values as high as $\sim 400 \text{ mg/L}$ were simulated for a cellulose diameter of 0.5 mm). For large-diameter cellulose particles ($> 8 \text{ mm}$), relatively low final acetate concentrations were obtained (i.e., $< 30 \text{ mg/L}$).

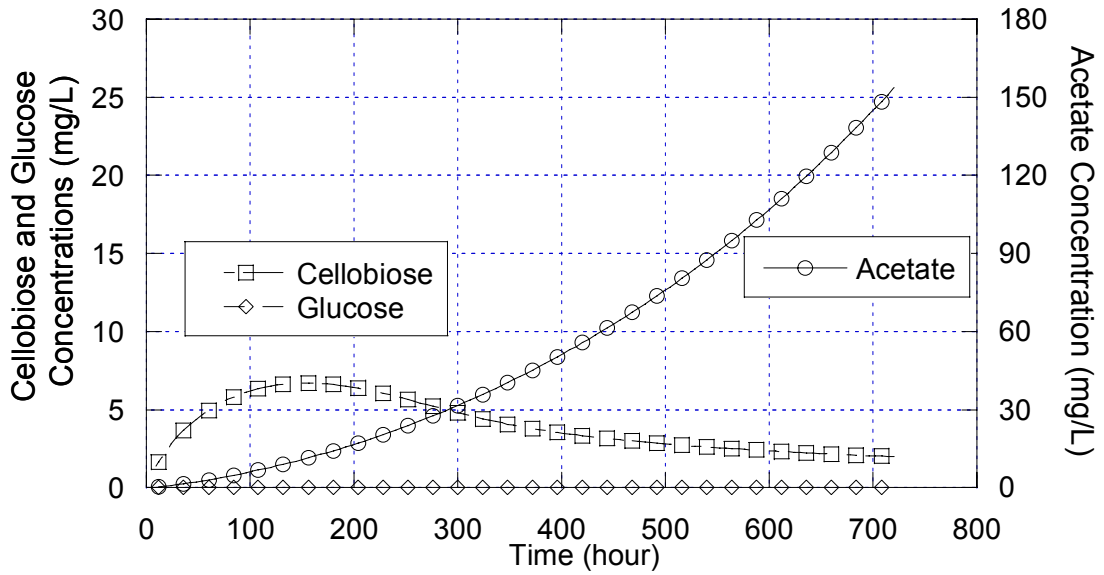


Figure 2. Production of cellobiose, glucose, and acetate from cellulose hydrolysis in batch experiment simulation extended to 720 hours; initial cellulose diameter 2.0 mm.

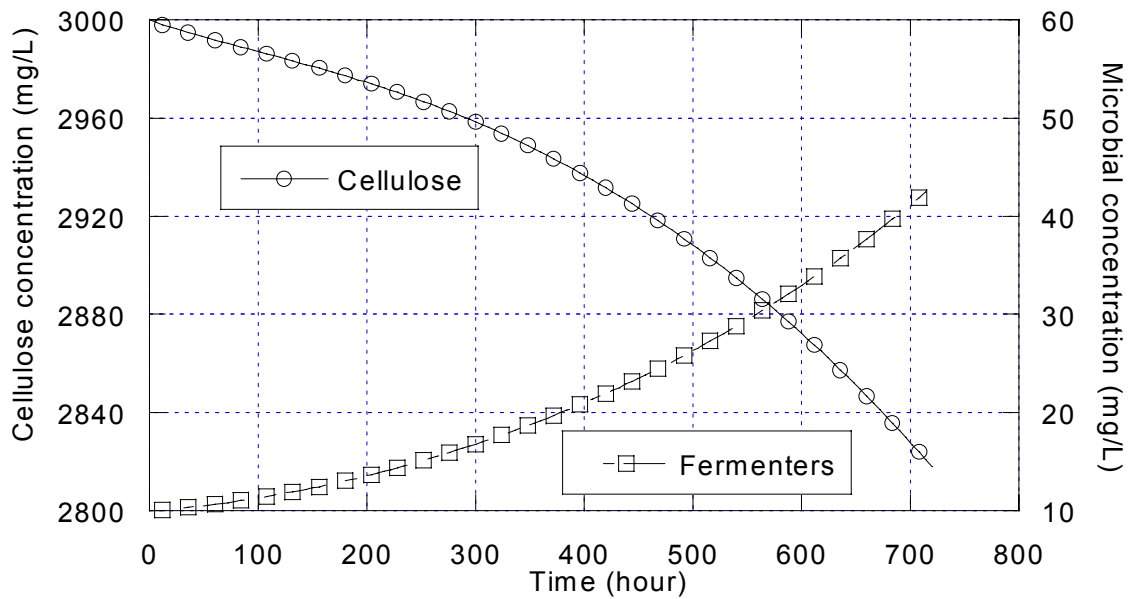


Figure 3. Cellulose hydrolysis, and microbial growth simulation in a batch experiment extended to 720 hours; initial cellulose diameter 2.0 mm.

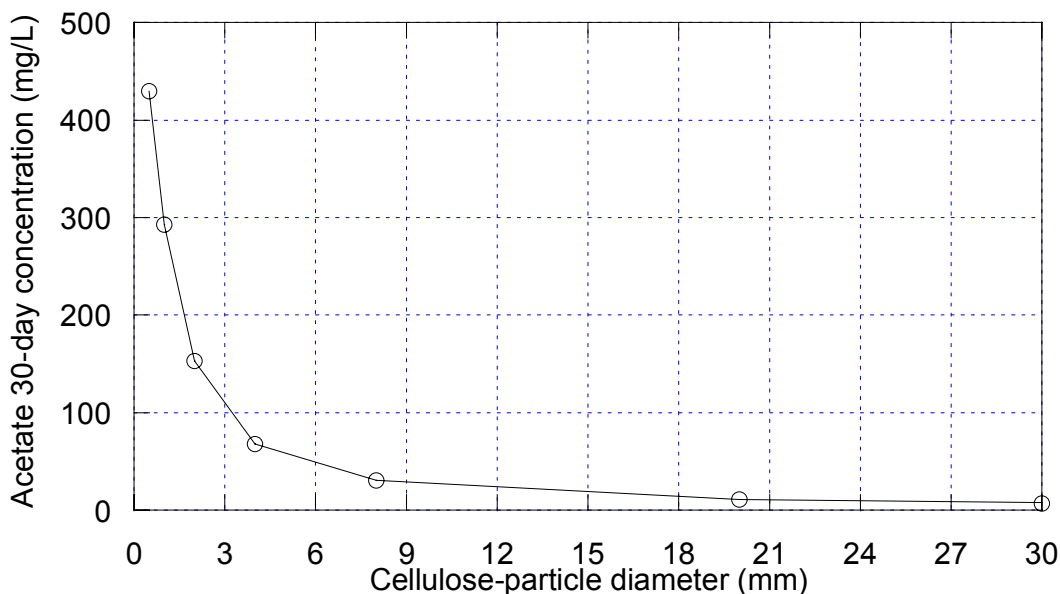


Figure 4. Estimate of final acetate concentration in 30-day batch equilibrations as a function of the initial cellulose particle size, for initial cellulose diameters ranging from 0.5 to 30 mm.

The values of acetate concentrations accumulated from cellulose hydrolysis in the batch simulations presented above (Figure 4) are of the same order of magnitude of acetate half-saturation constants for sulfate reducers and methanogens (i.e., 12 mg/L and 180 mg/L, respectively, Schönheit et al. 1982).

Kinetic Model of the Activity of Sulfate-Reducing Bacteria

Microbial populations in porous media are found predominantly attached to solid surfaces, forming discrete microcolonies or continuous biofilms. The simulation of bacterial activity can be approached using either a macroscopic model (Monod model) or microscopic models such as the biofilm model (Baveye and Valocchi 1989, Odencrantz et al. 1990). Although both approaches have been reviewed, the biofilm approach will be discussed here.

Microbial substrates have to be transferred from the bulk solution into the biofilm by inter-phase diffusion, and substrate mass balances within a biofilm must include the input of substrates provided by diffusion plus substrate uptakes linked to microbial growth.

A fully-penetrating biofilm is one with negligible substrate gradients within the biofilm, i.e., from the outer surface to the attachment surface (Rittman and McCarty 2001). Considering the

SRB biofilm to be mixed, i.e., (i) neglecting internal mass-transport resistances, and (ii) considering a spatially uniform bacterial activity within the biofilm, the biofilm modeling can be simplified considering a fully-penetrating biofilm (Figure 5).

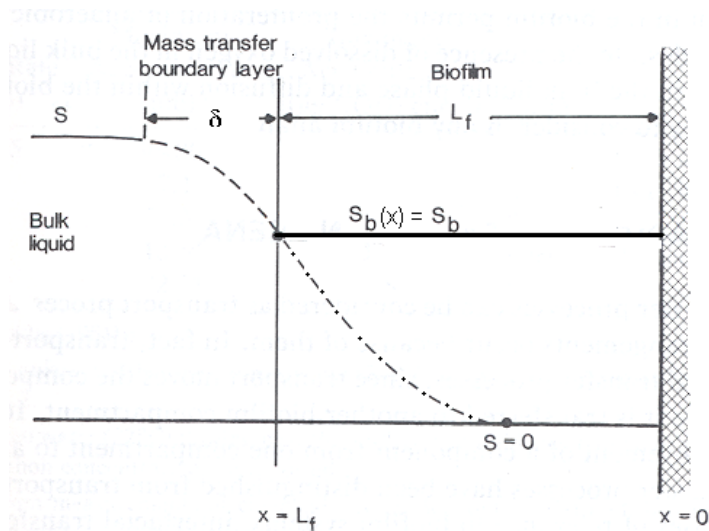


Figure 5. Schematic of substrate concentrations in the vicinity of, and within, a microbial biofilm, including: bulk liquid concentration (S), diffusion boundary layer thickness (δ), biofilm substrate concentration (S_b), and biofilm thickness (L_f) (modified from Characklis et al., 1990).

The biofilm under consideration in this study is necessarily multi-species, since one of the modeling objectives is to evaluate the competition between sulfate reduction and methanogenesis for the common substrate acetate (H_2 , as reported in Lovley et al. 1984, will be neglected).

Biofilm Characterization

The microbial biofilm is considered to totally cover the surface of inter-connected pores in the porous medium. For a medium in which the specific surface area (S_s) is defined as follows:

$$S_s = \frac{A}{V_{total}} \quad (14)$$

where, A is the surface area, and V_{total} is the total volume of porous medium, the biofilm volumetric content, θ_b is defined as follows:

$$\theta_b = \frac{V_{\text{biofilm}}}{V_{\text{total}}} = S_s L_f \quad (15)$$

where L_f is the biofilm thickness. If we define the volumetric content of biofilm in terms of the volume of the pore liquid (or volume of voids, in a saturated medium), then:

$$v_r = \frac{V_{\text{biofilm}}}{V_{\text{liquid}}} = \frac{S_s L_f}{\theta_w} \quad (16)$$

where v_r is the biofilm-to-mobile water volume ratio, and θ_w is the volumetric water content.

The bacterial density of a population “i” within the biofilm can be defined in terms of the mass of bacteria “i” in the biofilm phase divided by the biofilm volume as follows:

$$\rho_{b,i} = \frac{M_{b,i}}{V_{\text{biofilm}}} \quad (17)$$

This microscopic bacterial density is usually assumed constant (Baveye and Valocchi 1989), and biofilm growth will be assumed associated to an increase in biofilm thickness without changing the density.

A macroscopic microbial concentration could also be defined, i.e., the microbial concentration relative to the volume of the pore liquid (or voids). Neglecting the occurrence of any significant fraction of the bacterial population in the liquid (suspended) phase:

$$X_{b,i} = \frac{M_{b,i}}{V_{\text{liquid}}} = \frac{\rho_{b,i} \cdot S_s \cdot L_f}{\theta_w} \quad (18)$$

This equation shows that, with $\rho_{b,i}$ constant, biofilm growth (increase in $X_{b,i}$) is directly linked to an increase in biofilm thickness (L_f) as stated above. This macroscopic concentration based on the volume of the liquid phase is the one employed in modeling (equations representing

microbial dynamics) for that in this case the microbial population can be treated macroscopically in terms of a concentration that is analogous to that of any dissolved chemical species.

The concentration of a chemical species within the biofilm ($C_{b,i}$) is defined from the mass of the species within the biofilm phase ($M_{b,i}$) as:

$$C_{b,i} = \frac{M_{b,i}}{V_{\text{biofilm}}} \quad (19)$$

When diffusion occurs from the liquid to the biofilm phase, the transport of a small mass of substrate into the biofilm will be responsible for a large increase in $C_{b,i}$, since V_{biofilm} is very small.

Substrate Diffusion and Utilization in the Biofilm

The development of sulfate reduction and methanogenesis within the biofilm is limited by the substrates. Sulfate reducers require both acetate and sulfate, whereas methanogens depend only on acetate. Substrate mass transport by inter-phase diffusion from the free-liquid phase to the biofilm phase is responsible for substrate accumulation in the biofilm phase. The simplified biofilm in Figure 5 is assumed to have spatially-uniform concentrations of diffused acetate and sulfate, A_b , and SO_b , respectively.

Considering pure substrate diffusion (no utilization), an expression for the rate of change of acetate, for example, can be obtained as follows (analogous equations apply for sulfate):

$$\frac{dA_b}{dt} = \frac{D_a}{\delta L_f} (A - A_b) \quad (20)$$

where A is the acetate concentration in the free solution (supplied by cellulose hydrolysis), A_b is the acetate concentration within the film, δ is the thickness of the mass-transport boundary layer, and D_a is the inter-phase (boundary layer) diffusion coefficient for acetate. The rate of change in the free-liquid concentration (A) in Eq. 20 incorporates a term for acetate loss by diffusion:

$$\frac{dA}{dt} = -\frac{D_a}{\delta L_f} v_r (A - A_b) \quad (21)$$

Similar equations could be written for sulfate. For $A > A_b$, mass transport is towards the biofilm, and as $A_b \rightarrow A$, the rate of transfer approaches zero (concentrations approach an equilibrium value).

Substrate utilization within the biofilm due to the growth of sulfate reducers and methanogens is simulated using Michaelis-Menten kinetics. The following equations consider sulfate reduction and methanogenesis occurring in the same biofilm, and include substrate diffusion from the free-liquid phase. For the biofilm acetate concentration:

$$\begin{aligned} \frac{dA_b}{dt} = & \frac{D_a}{\delta L_f} (A - A_b) - 16.316\mu_{SRB}X_{SRB} \left(\frac{A_b}{K_{AS} + A_b} \right) \left(\frac{SO_b}{K_S + SO_b} \right) - \\ & 26.106\mu_M X_M \left(\frac{A_b}{K_{AM} + A_b} \right) \end{aligned} \quad (22)$$

where the numerical coefficients shown above are mass yield coefficients from the biochemical reactions, μ is the maximum specific microbial growth rate associated with each microbial population, and K is the half-saturation concentration for each microbial population growing on each substrate. For the substrate sulfate, the analogous expression is:

$$\frac{dSO_b}{dt} = \frac{D_{so}}{\delta L_f} (SO - SO_b) - 24.440\mu_{SRB}X_{SRB} \left(\frac{A_b}{K_{AS} + A_b} \right) \left(\frac{SO_b}{K_S + SO_b} \right) \quad (23)$$

Example of Numerical Simulation of the Activity of Sulfate Reducers

A Fortran-95 algorithm for the simulation of the mixed-population biofilm was developed. The values of variables X_{SRB} , X_M , A , SO , A_b , SO_b were simulated. Values of initial concentrations were selected, and are shown in Table 4. The model also included sulfide and methane production, which are not shown. The kinetic parameters required in the simulation are shown in Table 5.

Table 4. Initial concentrations considered in the example simulation.

Component	Initial Concentration (mg/L)	Component	Initial Concentration (mg/L)
SRB	10	Sulfate, biofilm	zero
Methanogens	10	Sulfide, free liquid	zero
Acetate, free liquid	50	Sulfide, biofilm	zero
Sulfate, free liquid	150	Methane	zero
Acetate, biofilm	zero		

The values of half-saturation constants were obtained from Schönheit et al. (1982) and Ingvorsen et al. (1984), and the maximum specific growth rates were selected by taking the average of some data collected for μ_{SRB} . The parameter “ $D_S/\delta L_f$ ” is analogous to parameters defined for Eqs. 22 and 23, and belongs to the equation for the diffusion of biofilm-generated sulfide towards the free solution (not shown).

For the parameter set and conditions reproduced in this numerical simulation, Figure 6 illustrates that acetate tends to be the limiting-growth substrate for both populations. The amount of sulfate reduction in the PRB system, and consequently the amount of AMD remediation achieved, will be surely lowered and limited by the presence of the competing population of methanogenic bacteria.

Table 5. Kinetic parameters in the example simulation.

Relevant Equation	Parameter	Adopted value
22	μ_{SRB}	0.1 hr^{-1}
22	K_{AS}	12 mg/L
22	K_{S}	20 mg/L
22	$D_{\text{A}}/\delta L_{\text{f}}$	0.05 hr^{-1}
22	μ_{M}	0.1 hr^{-1}
22	K_{AM}	180 mg/L
23	$D_{\text{SO}}/\delta L_{\text{f}}$	0.05 hr^{-1}
Not shown	$D_{\text{S}}/\delta L_{\text{f}}$	0.1 hr^{-1}

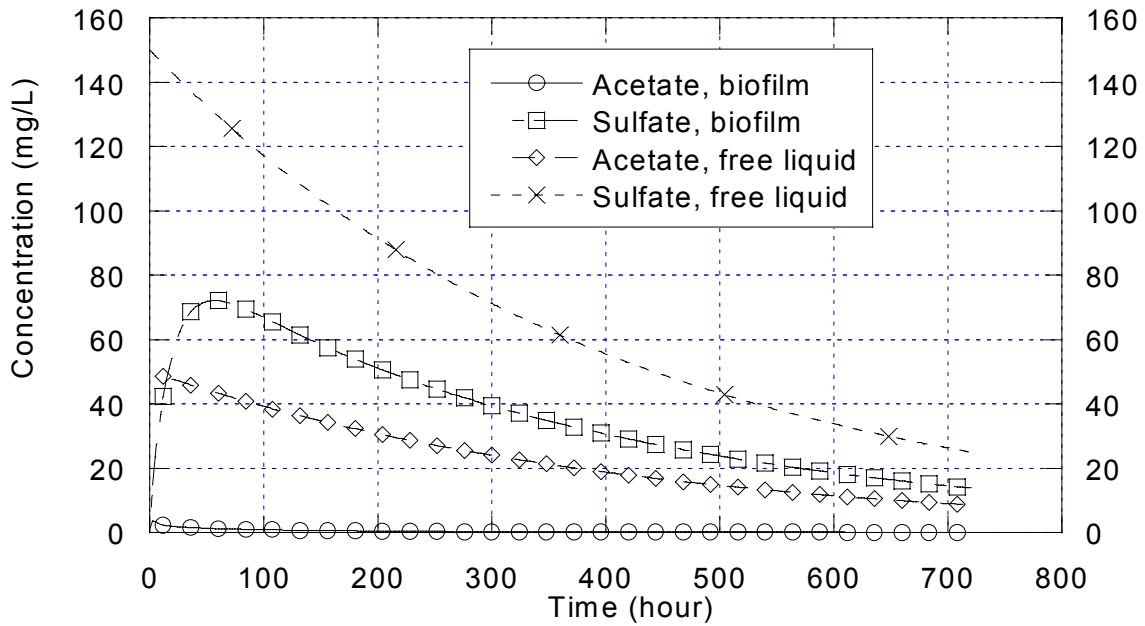


Figure 6. Example simulation of a mixed biofilm in which acetate becomes limiting to SRB growth due to the competition with and methanogenic bacteria.

Conclusions

The numerical simulation of the biochemical processes relevant to the study of permeable reactive barriers based on sulfate reduction for the amelioration of AMD revealed the existence of limiting factors that are often neglected in the PRB design. Such considerations include limitations in the final sulfate-reducing capacity of the barrier due to unfavorable kinetics of cellulose hydrolysis (with the initial cellulose particle size being a major factor), and due to the competition between sulfate reducers and methanogens for a common substrate.

In this research, different kinetic models have been considered and compared, in addition to the model focused in this paper, as well as the quantification of these biochemical processes under flow-and-transport scenarios (AMD transport through an aquifer intercepted by a PRB), in which the hydraulic residence time and characteristic reaction times (for instance the time associated with cellulose decomposition) have to be matched for ideal performance.

References

- Bain, J., Spink, L., Blowes, D., and Smyth, D. (2002). The removal of arsenic from groundwater using permeable reactive materials. Proceedings of the 9th International Conference on Tailings and Mine Waste, Fort Collins, CO, 27-30 January 2002.
- Baveye, P. and Valocchi, A. (1989). An evaluation of mathematical models of the transport of biologically reactive solutes in saturated soils and aquifers. *Water Resources Research*, 25(6):1413-1421. <http://dx.doi.org/10.1029/WR025i006p01413>
- Benner, S. G., Blowes, D. W., Gould, W. D., Herbert, R. B., and Ptacek, C. J. (1999). Geochemistry of a permeable reactive barrier for metals and acid mine drainage. *Environmental Science and Technology*, 33(16):2793-2799. <http://dx.doi.org/10.1021/es981040u>
- Chapra, S.C., and Canale, R.P. (2001). Numerical Methods for Engineers. 4th Edition, McGraw-Hill, New York, NY.
- Characklis, W. G., Turakhia, M. H., and Zilver, N. (1989). Transport and Interfacial Transfer Phenomena (chapter 9), in Biofilms, edited by W. G. Characklis, and K. C. Marshall, John Wiley and Sons, New York (NY).
- Drury, W. (2000). Modeling of sulfate reduction in anaerobic solid substrate bioreactors for mine drainage treatment. *Mine Water and the Environment*, 19(1):19-21. <http://dx.doi.org/10.1007/BF02687262>
- Gilbert, J.S., Wildeman, T.R., and Ford, K.L. (1999). Laboratory experiments designed to test the remediation properties of materials. Paper presented at the 1999 National Meeting of the American Society for Subsurface Mining and Reclamation, Scottsdale, AZ, 13-19 August 1999.

- Humphrey, A. E. (1979). The Hydrolysis of Cellulosic Materials to Useful Products (chapter 2), in Hydrolysis of Cellulose: Mechanisms of Enzymatic and Acid Catalysis. Advances in Chemistry Series, no. 181. American Chemical Society, <http://dx.doi.org/10.1021/ba-1979-0181.ch002>
- Ingvorsen, K., Zehnder, A. J., and Jorgensen, B. (1984). Kinetics of sulfate uptake by *Desulfobacter postgatei*. *Applied and Environmental Microbiology*, 47(2):403-408.
- Janssen, B.H. (1984). A simple method for calculating decomposition and accumulation of 'young' soil organic matter. *Plant and Soil*, 76:297-304. <http://dx.doi.org/10.1007/BF02205588>
- Ladisch, M. R., Hong, J., Voloch, M., and Tsao, G. T. (1981). Cellulase Kinetics, in Trends in the Biology of Fermentations for Fuels and Chemicals, edited by A. Hollaeder. Plenum Press, New York (NY). http://dx.doi.org/10.1007/978-1-4684-3980-9_5
- Lovley, D. R., Dwyer, D. F., and Klug, M. J. (1982). Kinetics analysis of competition between sulfate reducers and methanogens for hydrogen in sediments. *Applied and Environmental Microbiology*, 43(6):1373-1379.
- Ludwig, R. D., McGregor, R. G., Blowes, D. W., Benner, S. G., and Mountjoy, K. (2002). A permeable reactive barrier for treatment of heavy metals. *Ground Water*, 40(1):59-66. see below for link
- Odenchantz, J.E., Valocchi, A.J., and Rittmann, B.E. (1990). Modeling two-dimensional solute transport with different biodegradation kinetics. Proceedings of Petroleum Hydrocarbons and Organic Chemicals in Ground Water. October 31st to November 2nd 1990, Houston (TX).
- Rittman, B.E., and McCarty, P.L. (2001). Environmental Biotechnology: Principles and Applications. McGraw-Hill, New York, NY.
- Schönheit, P., Krisjansson, J. K., and Thauer, R. K. (1982). Kinetic mechanism for the ability of sulfate reducers to out-compete methanogens for acetate. *Archives of Microbiology*, 132(3):285-288. <http://dx.doi.org/10.1007/BF00407967>
- Waybrant, K. R., Blowes, D. W., and Ptacek, C. J. (1998). Selection of reactive mixtures for use in permeable reactive walls for treatment of mine drainage. *Environmental Science and Technology*, 32(13):1972-1979. <http://dx.doi.org/10.1021/es9703335>
- Waybrant, K. R., Ptacek, C. J., and Blowes, D. W. (2002). Treatment of mine drainage using permeable reactive barriers: column experiments. *Environmental Science and Technology*, 36(6):1349-1356. <http://dx.doi.org/10.1021/es010751a>
- Westrich, J.T., and Berner, R.A. (1984). The role of sedimentary organic matter in bacterial sulfate reduction: the G model tested. *Journal of Limnology and Oceanography*, 29(2):236-249. <http://dx.doi.org/10.4319/lo.1984.29.2.0236>

Ludwig, paper

<http://dx.doi.org/10.1111/j.1745-6584.2002.tb02491.x>